ChemComm
Chemical Communications

Accepted Manuscript

This article can be cited before page numbers have been issued, to do this please use: Y. Huang, Z. Cheng, Y. han, X. Gao, L. Qian, Y. Wen, X. Zhang and G. Liu, *Chem. Commun.*, 2020, DOI: 10.1039/D0CC05986B.

ROYAL SOCIETY OF CHEMISTRY

rsc.li/chemcomm

View Article Online
DOI: 10.1039/D0CC05986B

COMMUNICATION

Target-induced Molecular-switch on Triple-helix DNA-functionalized Carbon Nanotube for Simultaneous Visual Detection of Nucleic Acid and Protein

Received 00th January 20xx,
Accepted 00th January 20xx

DOI: 10.1039/x0xx00000x

Yan Huang[a,b], Zhihao Cheng[a], Rong Han[a], Xuan Gao[a], Lisheng Qian[a*], Yongqiang Wen[b], Xueji Zhang[b,c*], Guodong Liu[a*]

We report an easy and efficient approach based on target-induced molecular-switch on triple-helix DNA (THD)-functionalized carbon nanotube (CNT) for the simultaneous visual detection of nucleic acid and protein with a lateral flow nucleic acid biosensor. The assay had the capability to detect a minimum of 25 pM target DNA and 0.25 nM thrombin simultaneously within 20 min.

Rapid, sensitive, and specific detection of biomarkers including nucleic acids and proteins is very important for disease diagnosis, postoperative evaluation, drug discovery, and precision medicine. Most of the currently available diagnostic platforms detect proteins or nucleic acids separately[1]. Studies have shown that using a single platform to simultaneously identify two types of analytes in the same sample can not only bring economic benefits, but also be very helpful for precision medicine and early diagnosis, particularly when the sample size is limited[2-7]. Early methods of simultaneously detecting nucleic acids and proteins included multi-parameter cell analysis systems[8], combinations of DNA arrays and PCR, protein arrays and ELISA[9, 10]. However, these technologies and platforms required complicated and expensive instruments and professional operators. The following research aims at developing an integrated tool or platform for the rapid, simple, and cost-effective simultaneous detection of nucleic acids and proteins (SDNP) [11, 12].

In recent years, point-of-care (POC) biosensors for clinical diagnosis have developed rapidly[13]. Lateral flow strip biosensors (LFSB) were invented, in the 1960s, as an applicable tool to be widely used for protein POC detection [14-18]. This concept has been expanded by us[19, 20] and other groups[21, 22] to develop lateral flow nucleic acid biosensors (LFNAB). Most LFNABs use the base pairing principle of traditional double-stranded DNA structure to identify target molecules [19, 22-24]. However, triple-helix DNA (THD), based on Watson Crick and Hoogsteen base pairs, has recently received more attention because of its particular structure and properties[25-29]. In contrast to the known molecular beacons based on double-helix DNA and signal aptamers, THD displays special benefits, such as satisfying stability, high sensitivity and excellent preservation of the binding ability and specificity of the inside aptamer in the THD [30-33].

This study aims to design a new approach based on target-induced molecular-switch on triple-helix DNA (THD)-functionalized carbon nanotube (CNT) for simultaneous visual detection of nucleic acid and protein. **Figure 1** illustrates the principle and the potential results of simultaneous detecting DNA and protein using the THD-functionalized CNTs and LFNAB. The assay is based on the structure changes of the THDs on the CNT surface, due to the DNA-DNA hybridization and aptamer–protein reaction. DNA and thrombin were used as model targets to validate the feasibility of the design. The

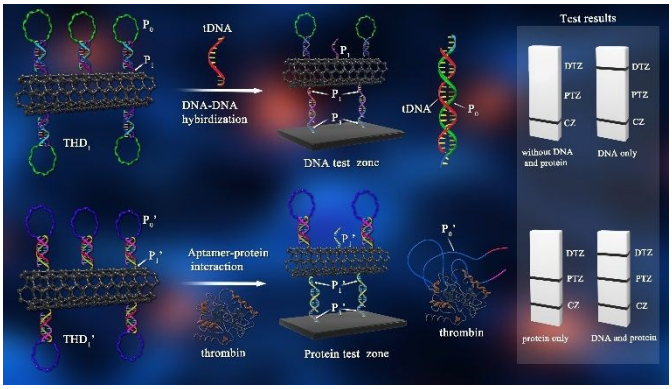

Fig. 1 Schematic illustration of the construction of the triple helix DNA-functionalized carbon nanotube and the strategy of simultaneous visual detection of the target DNA and thrombin. DTZ: DNA test zone; PTZ: protein test zone; CZ: Control zone; tDNA: target DNA.

[a] *Research Center for Biomedical and Health Science, Anhui Science and Technology University, Fengyang 233100, P. R. China. Email: qianls@ahstu.edu.cn and liugd@ahstu.edu.cn*
[b] *Research Center for Bioengineering and Sensing Technology, University of Science & Technology Beijing, Beijing, P. R. China. zhangxueji@ustb.edu.cn*
[c] *School of Biomedical Engineering, Shenzhen University Health Science Center, Shenzhen 518060, China.*

† Electronic Supplementary Information (ESI) available: Experimental section, characterization, polyacrylamide gel electrophoresis. See DOI: 10.1039/x0xx00000x

THD-CNT are prepared by the hybridization reactions between signal DNA probes (P_1) and assistant DNA probes (P_0) on the CNT surface. P_0 contains a central target specific sequence flanked by two arm segments, which hybridize with P_1 to form a trip helix. We design two signal DNA probes (P_1 and P_1') and two assistant DNA probes (P_0 and P_0') to form two THDs (THD1 and THD1'), which are used to recognize target DNA (tDNA) and thrombin, respectively. A thrombin aptamer sequence and tDNA complementary sequence are inserted into the central parts of P_0' and P_0, respectively. The sequences of all oligonucleotides in this study are listed in **Table S1** in Electronic Supplementary Information (ESI). The triple-helix structure of THDs leads the signal DNA probe P_0 to be protected. Due to the assistant DNA probe P_1 containing target specific sequence, presence of tDNA and thrombin induces the structure change of THDs resulting unprotected single-strand signal DNA probes on CNT surface, which are detected by a LFNAB to give visible black bands. The LFNABs with two test lines and one control line are prepared according to the reported procedure with slight modification (**Scheme S2, ESI**)[19, 20].

In the absence of both tDNA and thrombin, both the P_1 and P_1' signal probes on the CNT surface are protected due to the triple helix structure of THDs, and the CNT-THD conjugates will not be captured on the test lines during the test. In the presence of DNA and thrombin, the THD1 and THD1' on the CNT surface are disassembled because of the hybridization reactions between the tDNA and THD1, and the interactions between thrombin and THD1', resulting the P_1 and P_1' signal probes are unprotected. When the CNT-THD1 and CNT-THD1' conjugates flow over the test lines of LFNAB, the unprotected P_1 and P_1' on the CNT surface will hybridize with the pre-immobilized capture DNA probes P_3 and P_3' on the test lines, respectively, and thus the CNTs will be retained on the test lines. The accumulations of CNTs on the test lines result two black bands on the LFNAB. In order to validate the test, a couple of DNA probes, named as P_2 and P_4, are complementary each other, and used to prepare the CNT-P_2 conjugate and the control line of LFNAB, respectively. CNT-P_2 is premixed with the CNT-THD1 and CNT-THD1' before the test. During the test, the CNT-P_2 is captured by the P_4 on the control line for quality control. Therefore, in the absence of both tDNA and thrombin (control), only one single black band in the control zone is observed, showing the proper work of the LFNAB; in the presence of the tDNA and absence of thrombin, two black bands are observed in the DNA test zone and control zone; in the absence of tDNA and presence of thrombin, two black bands are observed in the protein test zone and control zone; in the presence of both the tDNA and thrombin, three black bands are observed. We monitor the test zones' color change as a qualitative judgement (Yes/No) and use a portable strip reader to read the greyscale of the black bands of the test zones to quantify the concentrations of DNA and protein.

To prepare the THD-functionalized CNTs, amine-modified signal DNA probes (P_1) were first immobilized on the shortened

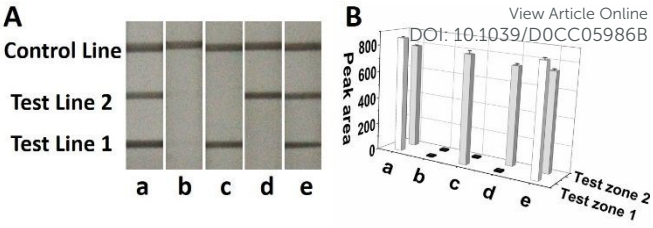

Fig. 2 (A) Photo pictures of LFNABs in the presence of (a) 1.5 μL CNT-P_1 + 1.5 μL CNT-P_1'; (b) 1.5 μL CNT-THD1 + 1.5 μL CNT-THD1'; (c) 1.5 μL CNT-THD1 + 1.5 μL CNT-THD1' + 2.5 nM tDNA; (d) 1.5 μL CNT-THD1 + 1.5 μL CNT-THD1' + 25 nM thrombin. (e) 1.5 μL CNT-THD1 + 1.5 μL CNT-THD1' + 2.5 nM tDNA + 25 nM thrombin and (B) the corresponding intensities of the test zones of the LFNAB.

CNT surface; assistant DNA probe P_0 was used to hybridize with the P_1 on the CNT to form the THD (**Scheme S1, ESI**).

We use ultrasound and mixed concentrated acid to shorten the carboxylated multi-walled CNTs. The shortened CNTs were characterized by transmission electron microscope (TEM) and Raman spectrum (**Figure S1A and S1B, ESI**). The carboxylic groups on the shortened CNT surface facilitate to immobilize the amine-modified P_1 on CNT by dehydration condensation reactions between carboxyl and amine groups. Polyacrylamide electrophoresis experiments confirmed the formation of CNT-P_1 conjugates (**Figure S2, ESI**). Two kinds of CNT-THD conjugates, named as CNT-THD1 and CNT-THD1' were prepared for the detection of DNA and protein, respectively.

To begin, the concept of target-induced molecular-switch on THD-functionalized CNTs was demonstrated by using signal DNA probe P_1 and THD conjugated CNT conjugates on the LFNAB device. **Figure 2Aa and 2Ab** display the images of the LFNABs after testing blank solutions (without tDNA and thrombin) using CNT-P (P_1, P_1' and P_2) and CNT-THD (THD1 and THD1') as conjugates, respectively. As expected, the signal probe (P_1 and P_1')-conjugated CNTs (CNT-P_1 and CNT-P_1') and control probe P_2-conjugated CNT (CNT-P_2) were captured on the test zones and control zone, respectively, due to the DNA-DNA hybridization reactions between P_1 and P_3 (DNA test zone), P_1' and P_3' (thrombin test zone), and P_2 and P_4 (control zone), resulting the characterized three black bands (**Figure 2Aa**). However, the THD-functionalized CNTs were not captured on the test zones and no test band was observed, indicating the signal probes (P_1 and P_1') were protected by the formed triple-helix structure of THDs (**Figure 2Ab**). **Figure 2A c-e** displays the typical images of LFNABs prepared with CNT-THDs after testing 2.5 nM tDNA, 25 nM thrombin and 2.5 nM tDNA+25 nM thrombin. One can see the black bands appeared on the test zones of LFNAB in the presence of tDNA /or thrombin. The above results indicate DNA or thrombin induced a structure change of THDs due to the DNA-DNA hybridization reactions or aptamer-thrombin interactions, leading to the signal probe P_1 (or P_1') unprotected on the CNT surface. **Figure 2B** shows the corresponding intensities of the

View Article Online
DOI: 10.1039/D0CC05986B

test lines of the LFNABs in the above five tests. The structure changes of THDs in the that the tDNA and thrombin can be easily differentiated from the other

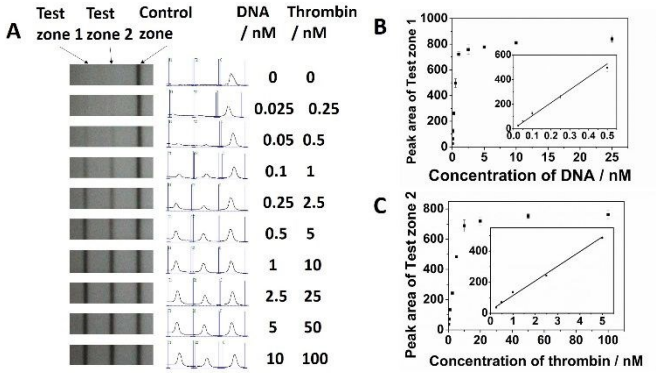

Fig. 3 (A) Photo pictures (left) and the corresponding optical responses of the LFNAB with an increasing tDNA concentration (0.025 to 10 nM) and thrombin concentration (0.25 to 100 nM). Typical dot plots and calibration curves (the inset) of the LFNABs in the presence of different concentrations of tDNA (B) and thrombin (C) under the optimal experimental conditions.

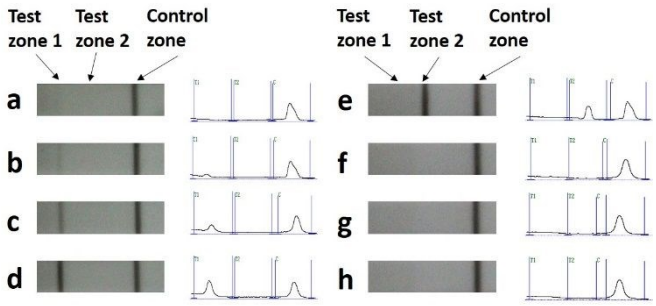

Fig. 4 Photo pictures and instrumental curves for the LFNAB of (a) noncomplementary DNA, (b) three-base-mismatched DNA, (c) one-base-mismatched DNA, and (d) complementary DNA, (e) thrombin, (f) IgG, (g) AFP and (h) CA-125. The concentrations of four DNAs are 1 nM. The concentrations of four proteins are 10 nM.

presence of tDNA and thrombin were confirmed with PAGE experiments (**Figure S3, ESI**).

Under optimal experimental conditions, the performance of the LFNAB was tested with the sample solutions containing different concentrations of tDNA and thrombin. **Figure 3A** shows the images of the NC membranes' function area (left) of LFNABs and the corresponding instrument reading (right). One can see the intensities and peak sizes of the test lines increased with the increase of both DNA and thrombin concentrations and saturated when the concentrations of DNA and thrombin were more than 0.5 nM and 10 nM, respectively (**Figure 3B, 3C**). This allowed us to carry out convenient qualitative and quantitative testing. The peak area value was linearly related to the DNA concentration in the range of 0.025 to 0.5 nM and the thrombin concentration in the range of 0.25 to 5 nM (**Figure 3B and 3C inset**). The detection limits of DNA and thrombin were approximately 0.024 nM and 0.216 nM (based on S/N = 3), respectively, which was two times better than the CNT-based traditional duplex DNA LFSB[34]. and 10 times better than the sandwich aptamer-gold nanoparticle based LFSB[15]. Besides, the detection limit of DNA and thrombin are better or comparable to the fluorescence-based THD method [33, 28]. In addition, calculated from the results obtained by measuring 0.1 nM DNA and 2.5 nM thrombin by six LFNABs, the relative standard deviations of testing DNA and thrombin were 8.5% and 6.9%, respectively (data not shown), indicating high reproducibility.

In order to determine whether the biosensor could selectively identify the targets, we tested four DNA sequences and four proteins under the same conditions, including noncomplementary DNA, one-base-mismatched DNA, three-base-mismatched DNA, complementary DNA target, thrombin, rabbit IgG, AFP and CA-125. The results indicated DNAs or proteins (**Figure 4**). The test line intensity of complementary DNA target was 3.42 times higher than that of the one-base-mismatched DNA, and 9.89 times higher than that of the three-base-mismatched DNA. The thrombin test displayed a bright black band on test zone 2 and no test band was observed for the other three proteins. Both these results indicated the good specificity of the LFNAB.

To summarize, we developed an easy and rapid assay to detect nucleic acids and proteins simultaneously on the basis of LFNAB and the target-induced molecular-switch on the triple helix DNA-functionalized CNT. A single-strand DNA target and thrombin were chosen to validate the feasibility. The triple-helix DNA-functionalized CNT conjugates were used as sensing elements. The structure change of triple-helix DNA on the CNT surface due to DNA hybridization and aptamer-target reaction produces the unprotected signal DNA probes on CNT, leading to a signal readout on the test zones of the LFNAB. The combination of this device, along with a portable strip reader, demonstrates the vast potential for on-site and POC quantitative/qualitative simultaneous investigation for disease-related DNA and protein biomarkers in biological samples. In addition, the method reported in this work is universal and can be expanded to detect other analytes by changing the sequence of assistant DNA probe. For example, the assistant DNA P_0 intermediate sequence can be changed to be a new sequence (DNA or aptamer), which is complementary to another target DNA or protein. The new approach thus provides a rapid, sensitive, low cost, and specific tool for the detection of nucleic acid and protein samples. It shows great promise for precision medicine and point-of-care diagnosis.

We acknowledge funding from the Natural Science Foundation of Anhui Province (1908085MB54), Key Research and Development Projects of Anhui Province (No. 202004a07020018), Major project of Anhui Provincial Department of Education (No. KJ2019ZD58), Wanjiang scholar Award of Anhui Province, National Natural Science Foundation of China (No. 21890740, 21890742, 21727815). Basic Research Business Fund of Central Universities (No. FRF-TP-18-020A1, FRF-BD-20-14A), China Postdoctoral Science Foundation (No. 2018 M631332).

Conflicts of interest

There are no conflicts to declare.

Notes and references

1. A. V. Ullal, V. Peterson, S. S. Agasti, S. Tuang, D. Juric, C. M. Castro and R. Weissleder, *Sci. Transl. Med.*, 2014, **6**, 219ra9.
2. W. Ma, M. Sun, P. Fu, S. Li, L. Xu, H. Kuang and C. Xu, *Adv. Mater.*, 2017, **29**, 1703410.
3. Scott, W. Alexander, Garimella, Viswanadham, Calabrese, M. Colin, Mirkin and A. Chad, *Bioconjug. Chem.*, 2016, 203-211.
4. X. Mao, A. Gurung, H. Xu, M. Baloda, Y. He, and G. liu, *Anal. Sci.*, 2014, 30, 637.
5. D. Falconnet, J. She, R. Tornay, E. Leimgruber, D. Bernasconi, L. Lagopoulos, P. Renaud, N. Demierre and P. van den Bogaard, *Anal. Chem.*, 2015, **87**, 1582-1589.
6. Y. Huang, W. Wen, D. Du, X. Zhang, S. Wang and Y. Lin, *Biosens. Bioelectro.*, 2014, **61**, 598-604.
7. A. P. Frei, F. A. Bava, E. R. Zunder, E. W. Hsieh, S. Y. Chen, G. P. Nolan and P. F. Gherardini, *Nat. Methods*, 2016, **13**, 269-275.
8. H. Crissman and J. Steinkamp, *J. Cell Biol.*, 1973, **59**, 766.
9. E. Flamini, L. Mercatali, O. Nanni, D. Calistri, R. Nunziatini, W. Zoli, P. Rosetti, N. Gardini, A. Lattuneddu, G. M. Verdecchia and D. Amadori, *Clin. Cancer Res.*, 2006, **12**, 6985-6988.
10. T. Ideker, V. Thorsson, J. A. Ranish, R. Christmas, J. Buhler, J. K. Eng, R. Bumgarner, D. R. Goodlett, R. Aebersold and L. Hood, *Science*, 2001, **292**, 929-934.
11. Harper, C. Jason, Polsky, Ronen, Wheeler, R. David, Dirk, M. Shawn, Brozik and M. Susan, *Langmuir*, 2007,**23**, 8285-8287.
12. J. Ladd, A. D. Taylor, M. Piliarik, J. Homola and S. Jiang, *Anal. Chem.*, 2008, **80**, 4231-4236.
13. C. Parolo and A. Merkoci, *Chem. Soc. Rev.*, 2013, **42**, 450-457.
14. H. Xu, J. Chen, J. Birrenkott, J. X. Zhao, S. Takalkar, K. Baryeh and G. Liu, *Anal. Chem.*, 2014, **86**, 7351-7359.
15. H. Xu, X. Mao, Q. Zeng, S. Wang, A. N. Kawde and G. Liu, *Anal. Chem.*, 2009, **81**, 669-675.
16. G. Liu, Y. Y. Lin, J. Wang, H. Wu, C. M. Wai and Y. Lin, *Anal. Chem.*, 2007, **79**, 7644-7653.
17. J. Deng, M. Yang, J. Wu, W. Zhang and X. Jiang, *Anal. Chem.*, 2018, **90**, 9132-9137.
18. J. Hu, Z. L. Zhang, C. Y. Wen, M. Tang, L. L. Wu, C. Liu, L. Zhu and D. W. Pang, *Anal. Chem.*, 2016, **88**, 6577-6584.
19. X. Mao, Y. Ma, A. Zhang, L. Zhang, L. Zeng and G. Liu, *Anal. Chem.*, 2009, **81**, 1660-1668.
20. Y. He, K. Zeng, A. S. Gurung, M. Baloda, H. Xu, X. Zhang and G. Liu, *Anal. Chem.*, 2010, **82**, 7169-7177.
21. J. R. Choi, Z. Liu, J. Hu, R. Tang, Y. Gong, S. Feng, H. Ren, T. Wen, H. Yang, Z. Qu, B. Pingguan-Murphy and F. Xu, *Anal. Chem.*, 2016, **88**, 6254-6264.
22. X. Wang, N. Choi, Z. Cheng, J. Ko, L. Chen and J. Choo, *Anal. Chem.*, 2017, **89**, 1163-1169.
23. A. Abi and E. E. Ferapontova, *J. Am. Chem. Soc.*, 2012, **134**, 14499-14507.
24. T. A. Feagin, D. P. Olsen, Z. C. Headman and J. M. Heemstra, *J. Am. Chem. Soc.*, 2015, **137**, 4198-4206.
25. F. McKenzie, K. Faulds, D. Graham, *Chem. Commun.* 2008, 2367-2369.
26. V. V. Filichev, I. V. Astakhova, A. D. Malakhov, V. A. Korshun, E. B. Pedersen, *Chemistry* 2008, **14**, 9968-9980.
27. J. Zheng, A. Jiao, R. Yang, H. Li, J. Li, M. Shi, C. Ma, Y. Jiang, L. Deng and W. Tan, *J. Am. Chem. Soc.*, 2012, **134**, 19957-19960.
28. J. Zheng, J. Li, Y. Jiang, J. Jin, K. Wang, R. Yang and W. Tan, *Anal. Chem.*, 2011, **83**, 6586-6592.
29. Z. Zhang, Y. Wang, N. Zhang, S. Zhang, *Chem. Sci.,* 2016, **7**, 4184-4189.
30. J. Zheng, Y. Hu, J. Bai, C. Ma, J. Li, Y. Li, M. Shi, W. Tan and R. Yang, *Anal. Chem.*, 2014, **86**, 2205-2212.
31. S. Ye, Y. Wu, W. Zhang, N. Li, B. Tang, *Chem. Commun.,* 2014, **50**, 9409-9412.
32. E. Xiong, Z. Li, X. Zhang, J. Zhou, X. Yan, Y. Liu and J. Chen, *Anal. Chem.*, 2017, **89**, 8830-8835.
33. P. Tang, J. Zheng, J. Tang, D. Ma, W. Xu, J. Li, Z. Cao, R. Yang, *Chem. Commun.,* 2017, **53**, 2507-2510.
34. W. Qiu, H. Xu, S. Takalkar, A. S. Gurung, B. Liu, Y. Zheng, Z. Guo, M. Baloda, K. Baryeh and G. Liu, *Biosens. Bioelectron.*, 2015, **64**, 367-372.

Entry for the Table of Contents

View Article Online
DOI: 10.1039/D0CC05986B

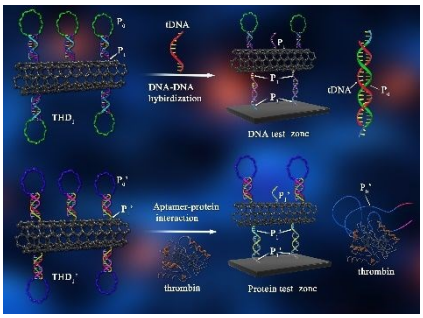

The structure of triple-helix DNA (THD) leads the signal DNA probes to be protected on the carbon nanotube (CNT) surface. Due to the assistant DNA probe containing target specific sequences, presence of target DNA and thrombin induces the structure change of THDs resulting unprotected single-strand signal DNA probes on CNTs, which are detected by a lateral flow nucleic acid strip biosensor to give visible black bands.